

Supporting Information

Fluorophore targeting to cellular proteins via enzyme-mediated azide ligation and strain-promoted cycloaddition

Jennifer Z. Yao,[†] Chayasith Uttamapinant,[†] Andrei Poloukhine,[‡] Jeremy M. Baskin,[§] Julian A. Codelli,[§] Ellen M. Sletten,[§] Carolyn R. Bertozzi,^{§,||,⊥} Vladimir V. Popik,[‡] and Alice Y. Ting^{*,†}

[†]Department of Chemistry, Massachusetts Institute of Technology, 77 Massachusetts Avenue.
Cambridge, Massachusetts 02139

[‡]Department of Chemistry, University of Georgia, 212 Carlton Street. Athens, Georgia 30602

[§]Departments of Chemistry and ^{||} Molecular and Cell Biology and Howard Hughes Medical
Institute, University of California, Berkeley, California 94720

[⊥]The Molecular Foundry, Lawrence Berkeley National Laboratory, Berkeley, California 94720

E-mail: ating@mit.edu

Contents of Supporting Information

Supporting Figure 1: Optimization of probe loading and washout steps

Supporting Figure 2: Identification of the best LplA mutant/azide substrate pair for intracellular protein labeling

Supporting Figure 3: *In vitro* characterization of azide 9 ligation catalyzed by ^{W37I}LplA

Supporting Figure 4: Characterization of intracellular labeling yields

Supporting Figure 5: Analysis of background labeling by cyclooctyne-fluorophore conjugates

Supporting Figure 6: Cell surface protein labeling with DIBO-Alexa Fluor 647 and DIBO-biotin

Supporting Methods

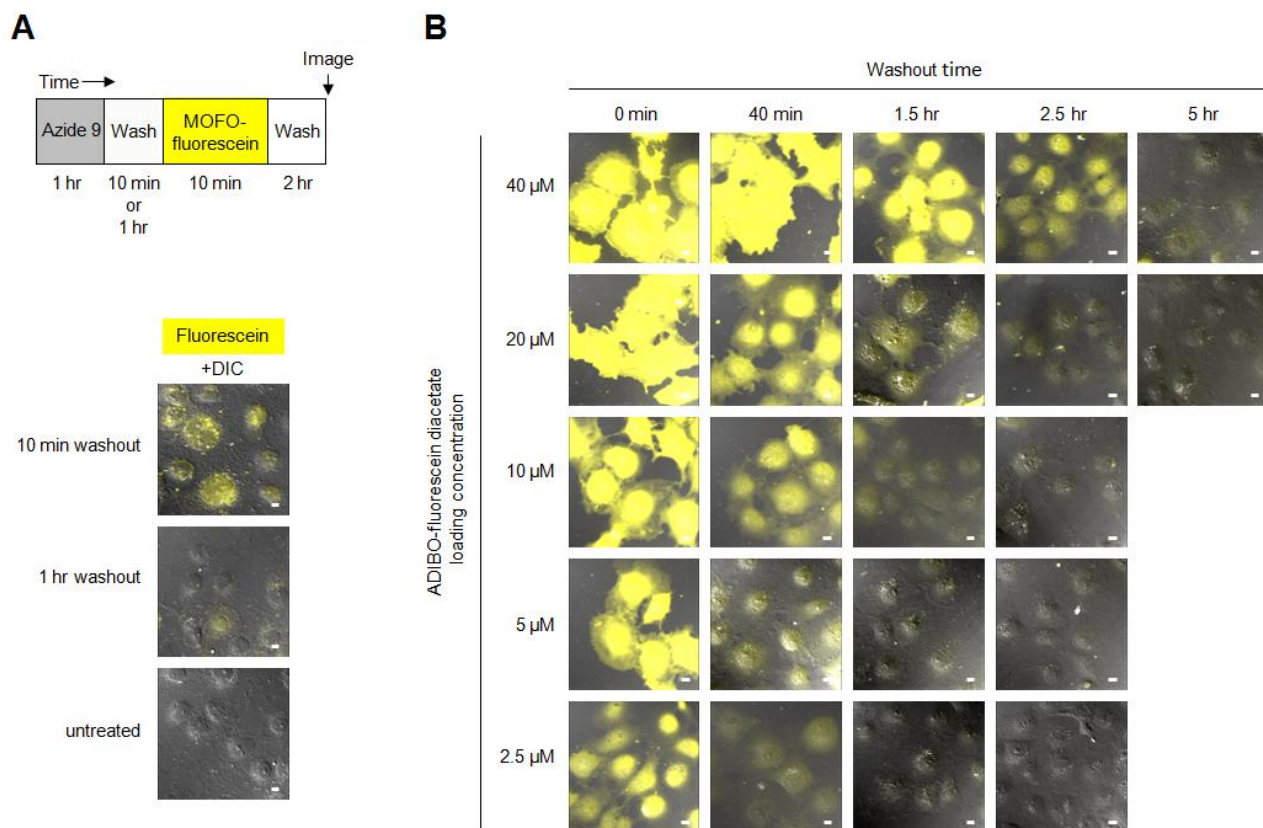


Figure S1. Optimization of probe loading and washout steps. **(A)** Determination of azide 9 washout time. Following the protocol shown at the top, untransfected HEK cells were incubated with 200 μ M azide 9 for 1 hr, then washed for either 10 min or 1 hr, before adding 10 μ M MOFO-fluorescein diacetate for 10 min. Cells were imaged after a 2 hr wash. The images show that fluorescein background is almost as low with 1 hr azide washout, as in cells not treated with azide at all. **(B)** Two-dimensional optimization of ADIBO-fluorescein diacetate loading concentration and washout time. Various amounts of ADIBO-fluorescein were loaded into untransfected COS-7 cells for 10 min at 37 °C. Various washout times were tested, ranging from 0 to 5 hr. Fluorescein images are shown with DIC overlay. All scale bars, 10 μ m. Based on this data, we selected 10 μ M ADIBO-fluorescein and 2 - 2.5 hr washout time for subsequent experiments.

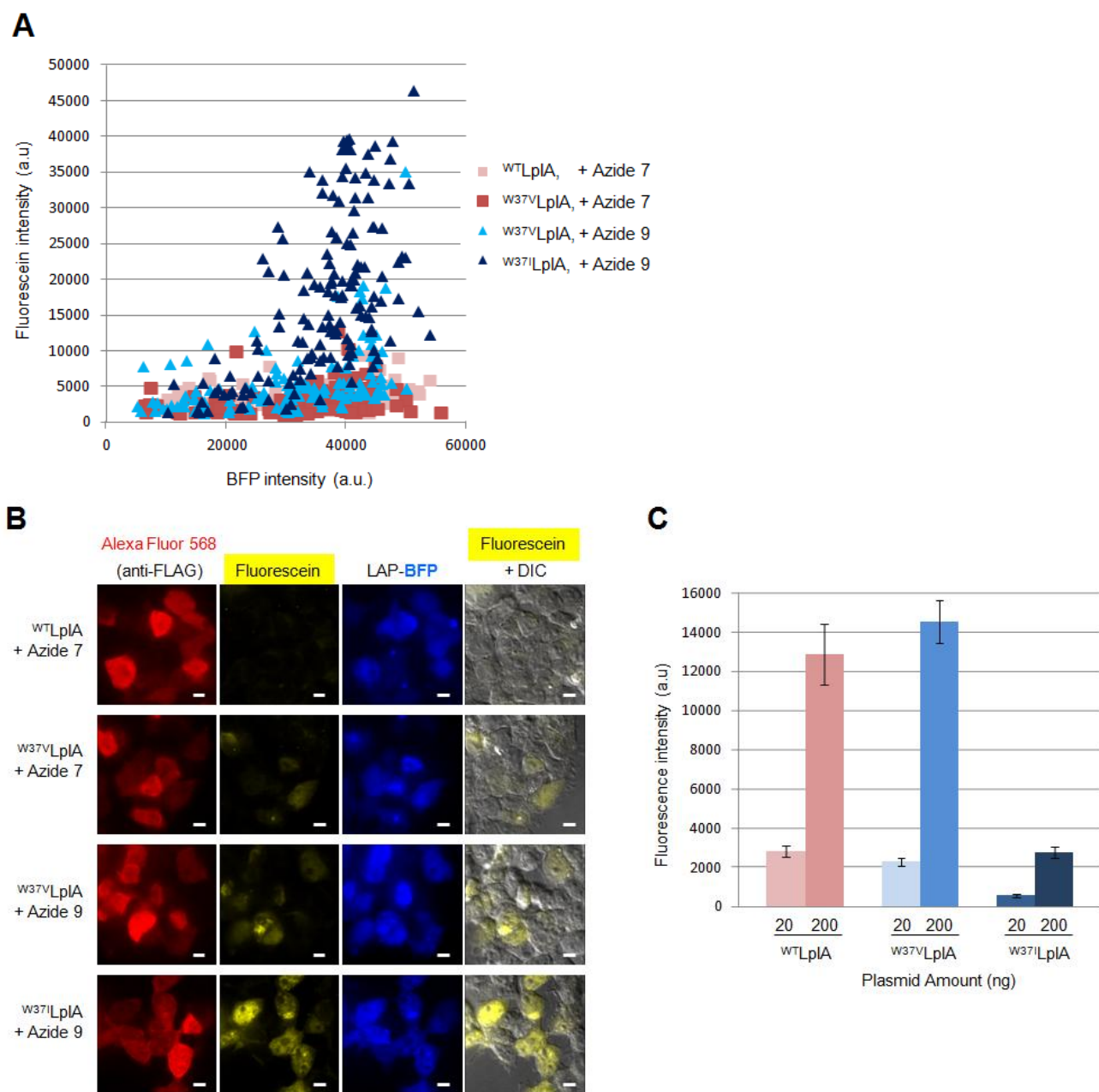


Figure S2. Identification of the best LplA mutant/azide substrate pair for intracellular protein labeling. **(A)** Quantitation of data shown in Figure 2B. For each condition, the mean fluorescein intensity was plotted against the mean BFP intensity, for >100 single cells. Fluorescein ligation yield is highest for the W^{37I}LplA/azide 9 combination. **(B)** A repeat of Figure 2B, except that cells were fixed and stained with anti-FLAG antibody to visualize FLAG-tagged LplA expression levels. To obtain matched LplA expression levels here and in Figure 2B, ten-fold more W^{37I}LplA plasmid was introduced compared to WT LplA and W^{37V}LplA plasmids. All scale bars, 10 μ m. **(C)** Graph showing quantitation of LplA mutant expression levels in cells. Mean Alexa Fluor 568 intensities (anti-FLAG staining) for > 30 single cells from each condition were averaged and graphed here.

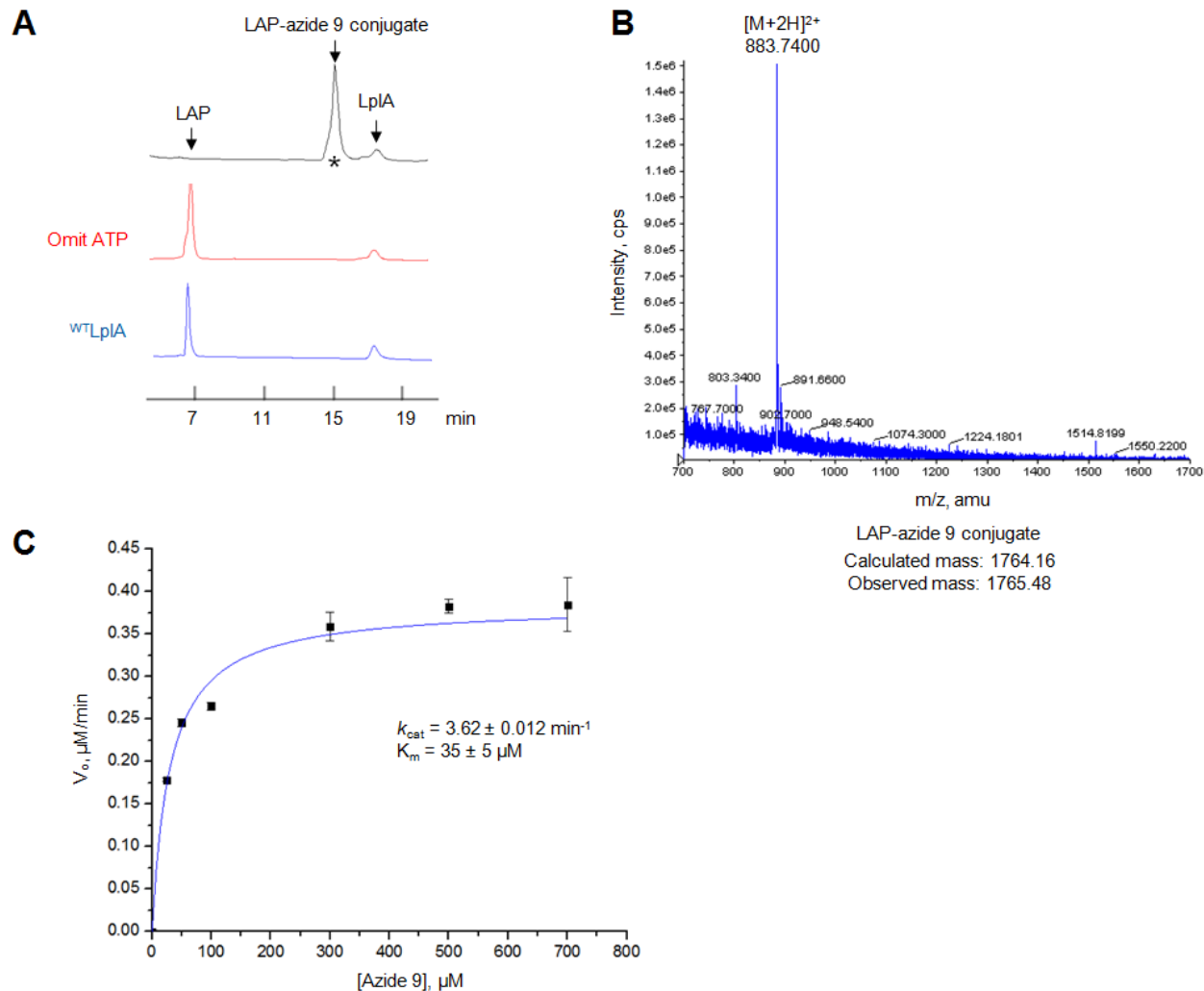


Figure S3. *In vitro* characterization of azide 9 ligation catalyzed by ^{W371}LpIA. **(A)** HPLC trace showing LAP conversion to LAP-azide 9 conjugate, catalyzed by ^{W371}LpIA (black trace). Negative controls are shown with ATP omitted (red trace) and ^{W371}LpIA replaced by wild-type LpIA (blue trace). Reactions were performed for 2 hr with 1 μM LpIA, 300 μM LAP, and 500 μM azide 9. **(B)** ESI mass spectrometric analysis of LAP-azide 9 covalent adduct (starred product peak in (A)). **(C)** Michaelis-Menten curve and kinetic parameters for azide 9 ligation onto LAP, catalyzed by 100 nM ^{W371}LpIA. Initial rates (V_o) were measured using the HPLC assay in (A) with 600 μM LAP and 25-700 μM azide 9. Each V_o value was measured in triplicate. Error bars, ± 1 s.d.

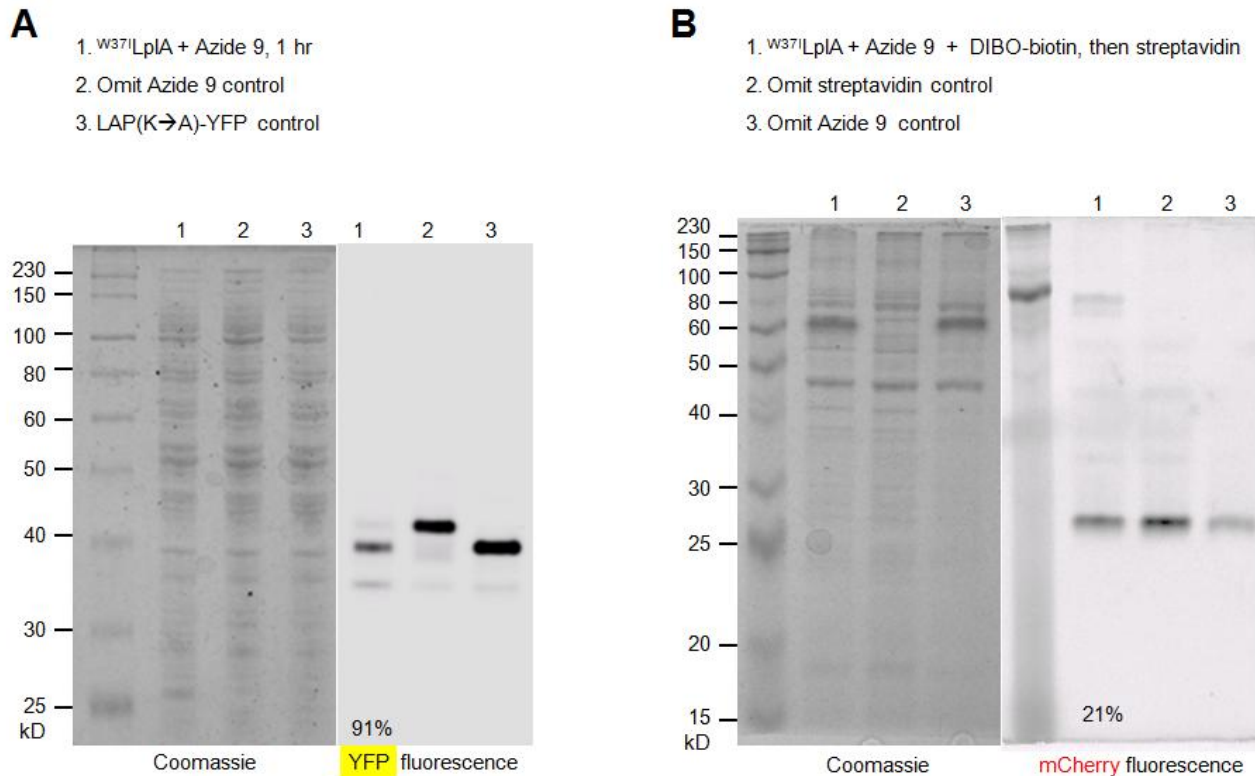
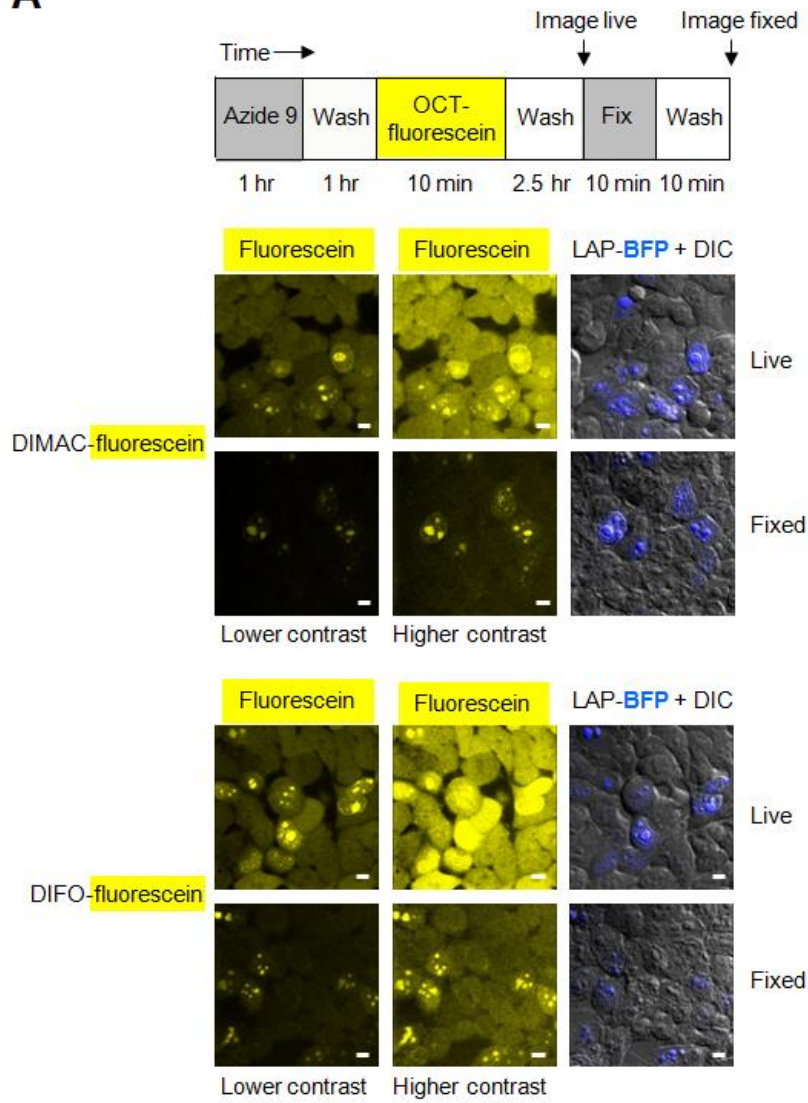


Figure S4. Characterization of intracellular labeling yields. **(A)** Gel-shift analysis of azide ligation in cells. Lane 1 is the same as lane 3 in Figure 2C. Lane 2 shows a negative control with azide 9 omitted. Lane 3 shows a negative control with the lysine in LAP mutated to alanine. This mutation causes LAP-YFP to shift downward in the 12% polyacrylamide native gel because it removes one positive charge from LAP-YFP. Similarly, labeling of the lysine of LAP causes a downward shift because the positive charge of lysine is converted to a neutral amide. Estimated percent conversions to product are given at the bottom of the YFP fluorescence gel image. **(B)** Streptavidin-shift analysis of two-step labeling yield in cells. HEK cells co-expressing W371 LpIA and LAP-mCherry were labeled with azide 9 for 1 hr, then DIBO-biotin for 10 min. After cell lysis, excess streptavidin protein (56 kDa) was added to shift the molecular weight of biotinylated LAP-mCherry (27 kDa). Coomassie and mCherry fluorescence visualization are shown for lysates run on a 12% SDS-polyacrylamide gel. Lane 2 shows a negative control with streptavidin omitted. Lane 3 shows omission of azide 9.

A

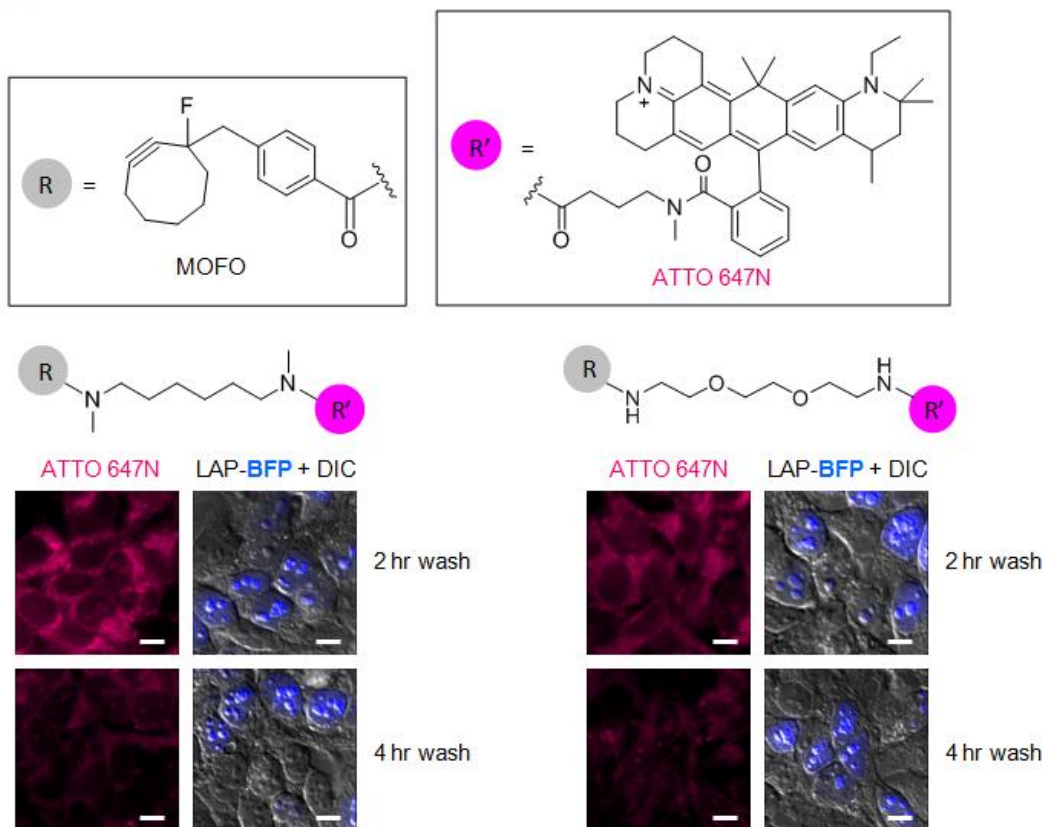
B

Figure S5. Analysis of background labeling by cyclooctyne-fluorophore conjugates. **(A)** Samples from Figure 3A labeled with DIMAC-fluorescein and DIFO-fluorescein were re-imaged after cell fixation. Labeling and imaging protocol is given at the top. Non-specific fluorescence is much reduced after fixation for DIMAC-fluorescein but not as much for DIFO-fluorescein. **(B)** Comparison of two different linker structures for MOFO-ATTO 647N. Conjugates were synthesized with either an N,N'-dimethyl-1,6-hexanediamine linker (left) or a polyethylene glycol linker (right). Labeling was performed on HEK cells expressing ^{W371}Lp1A and nuclear-localized LAP-BFP as described in Figure 3A. Images are shown after the indicated fluorophore washout times. Specific labeling is detectable, particularly in the nucleoli of transfected cells, but the images are dominated by the non-specific signal in these experiments. All scale bars, 10 μm.

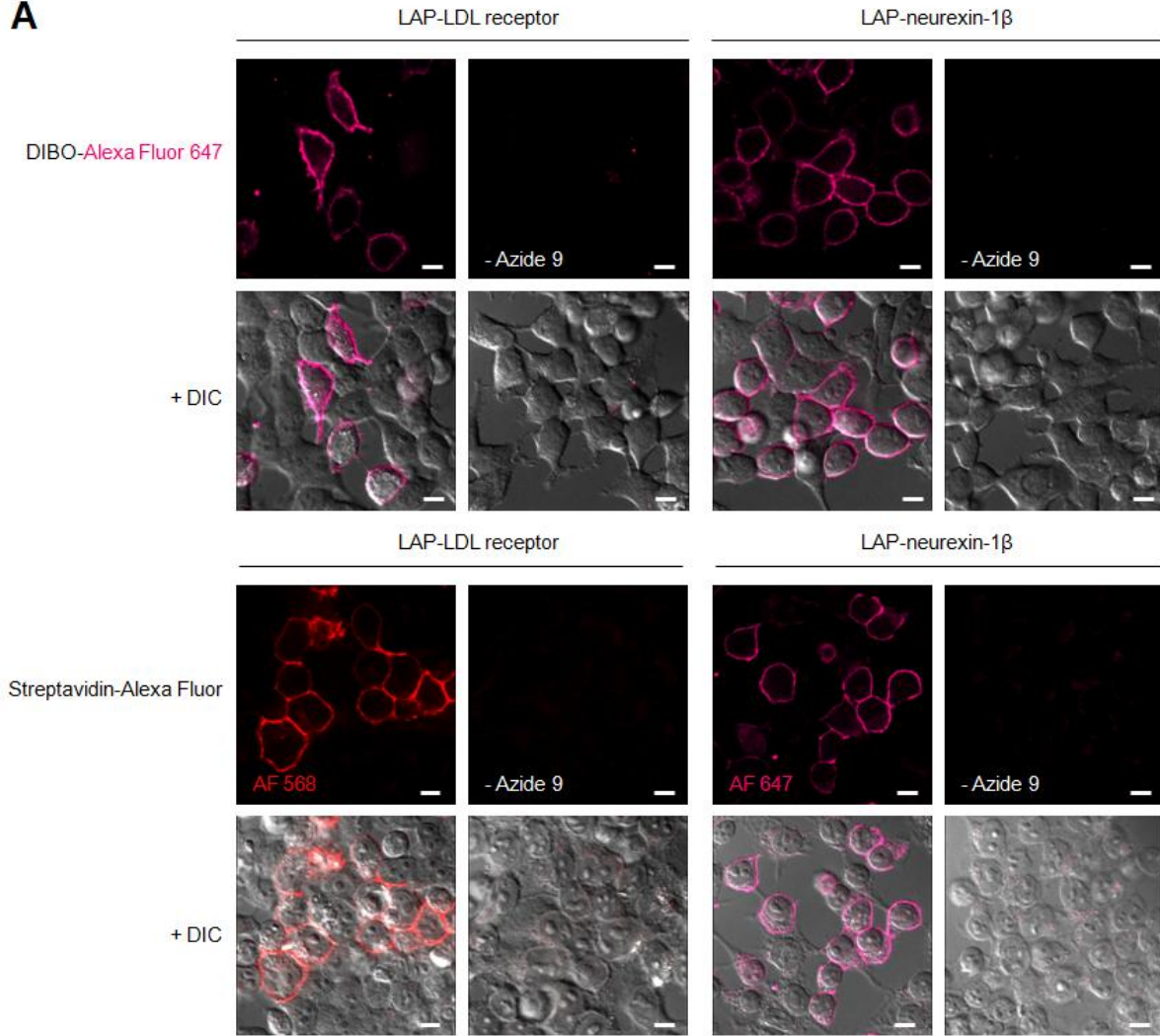
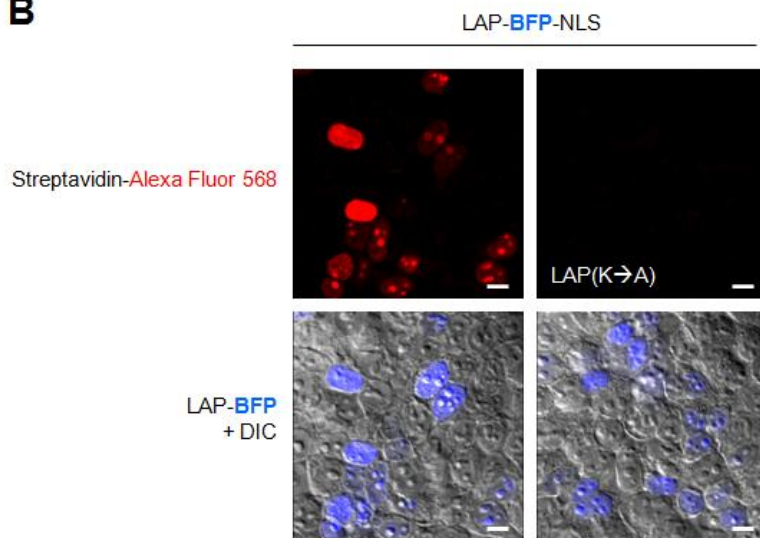
A**B**

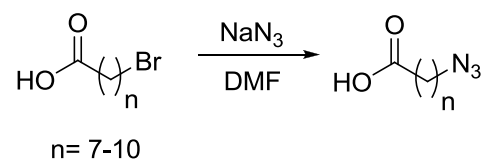
Figure S6. Cell surface protein labeling with DIBO-Alexa Fluor 647 and DIBO-biotin (both commercially available from Life Technologies). **(A)** HEK cells expressing LAP-LDL receptor (low density lipoprotein receptor) or LAP-neurexin-1 β were labeled by first adding purified ^{W371}LpIA enzyme and azide 9 to the cell medium for 20 min. After 5 min of washing, DIBO-Alexa Fluor 647 or DIBO-biotin was added for 10 min. DIBO-biotin was detected by staining with streptavidin-Alexa Fluor conjugate. Negative controls are shown with azide 9 omitted. **(B)** DIBO-biotin labeling could also be detected on intracellular proteins, after cell fixation and staining with streptavidin. HEK cells expressing ^{W371}LpIA and nuclear-targeted LAP-BFP-NLS were labeled live with azide 9 and then DIBO-biotin. Thereafter, cells were fixed and labeled proteins were detected by staining with streptavidin-Alexa Fluor 568 conjugate. A negative control is shown with an alanine mutation in LAP. All scale bars, 10 μ m.

Supporting Methods

General synthetic methods

All reagents were the highest grade available and purchased from Sigma-Aldrich, Anaspec, Thermal Scientific, TCI America, Alfa Aesar, or Life Technologies and used without further purification. Anhydrous solvents were drawn from Sigma-Aldrich SureSeal bottles. Analytical thin layer chromatography was performed on 0.25 mm silica gel 60 F₂₅₄ plates and visualized under short or long wavelength UV light, or after staining with bromocresol green or ninhydrin. Flash column chromatography was carried out using silica gel (ICN SiliTech 32-63D). Mass spectrometric analysis was performed on an Applied Biosystems 200 QTRAP mass spectrometer using electrospray ionization. HPLC analysis and purification were performed on a Varian Prostar Instrument equipped with a photo-diode-array detector. A reverse-phase Microsorb-MV 300 C18 column (250 × 4.6 mm dimension) was used for analytical HPLC. NMR spectra were recorded on a Bruker AVANCE 400 MHz instrument.

Synthesis of alkyl azide probes



To a solution of the corresponding bromoalkanoic acid (~1 g, 5 mmol) in 10 mL N,N-dimethylformamide (DMF) was added sodium azide (~0.5 g, 7.5 mmol). The mixture was allowed to stir at room temperature overnight. The progress of the reaction was monitored by thin layer chromatography (1:2 hexanes:ethyl acetate) followed by bromocresol green stain. Upon completion, DMF was removed under reduced pressure. The resulting residue was re-dissolved in 15 mL of 1 M HCl and extracted with ethyl acetate (3 x 15 mL). The organic layer was dried over magnesium sulfate, then filtered. After removal of ethyl acetate *in vacuo*, the crude product was purified by silica gel chromatography (solvent gradient 0-15% ethyl acetate in hexanes) to afford the corresponding azidoalkanoic acid as clear or pale yellow oil. Yields ranged from 50-70%.

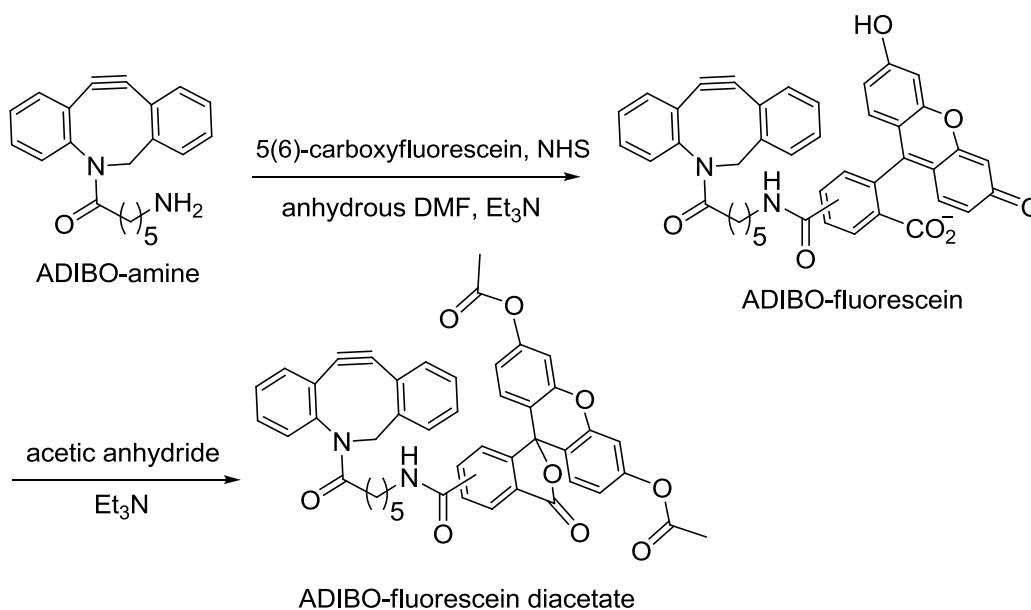
Characterization of n=7 azide (8-azidooctanoic acid). $^1\text{H NMR}$ (CDCl_3): 11.87 (s, 1H) 3.20 (t, 2H, $J = 6.9$), 2.28 (t, 2H, $J = 7.5$), 1.56 (m, 5H), 1.33 (m, 5H). ESI-MS calculated for $[\text{M-H}]^-$: 184.11; observed 183.66.

Characterization of n=8 azide (9-azidononanoic acid). $^1\text{H NMR}$ (CDCl_3) 3.22 (t, 2H, $J = 6.9$), 2.30, (t, 2H, $J = 7.5$), 1.60 (m, 5H), 1.29 (m, 7H). ESI-MS calculated for $[\text{M-H}]^-$: 198.12; observed 198.65.

Characterization of n=9 azide (10-azidodecanoic acid). $^1\text{H NMR}$ (CDCl_3): 3.23 (t, 2H, $J = 6.9$), 2.28 (t, 2H, $J = 7.5$), 1.53 (m, 5H), 1.31 (m, 9H). ESI-MS calculated for $[\text{M-H}]^-$: 212.14; observed 212.28.

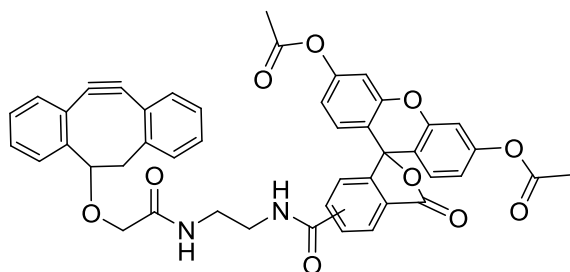
Characterization of n=10 azide (11-azidoundecanoic acid) $^1\text{H NMR}$ (CDCl_3) 3.27 (t, 2H, $J = 7.1$), 2.39, (t, 2H, $J = 7.5$), 1.65 (m, 5H), 1.20 (m, 11H). ESI-MS calculated for $[\text{M-H}]^-$: 226.16; observed 226.12.

Synthesis of ADIBO- and DIBO-fluorophore conjugates



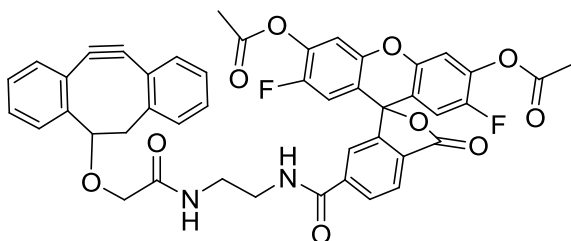
ADIBO-fluorescein diacetate The synthesis of aza-dibenzocyclooctyne-amine (ADIBO-amine) has been previously described.¹ To a solution of ADIBO-amine (3 mg, 9 μmol) in anhydrous DMF (500 μL) was added triethylamine (Et_3N , 3.8 μL , 27 μmol) and 5,6-carboxyfluorescein succinimidyl ester (NHS) (9.9 μmol , AnaSpec). The reaction was allowed to proceed for 10 hr at room temperature. Solvent was then removed under reduced pressure. The residue was subsequently

ADIBO-ATTO 647N, ADIBO-ATTO 655 ADIBO conjugates to ATTO 647N and ATTO 655 were synthesized in a similar manner from ADIBO-amine.¹ ATTO 647 NHS ester (Sigma-Aldrich) and ATTO 655 NHS ester (Sigma Aldrich) were used. Conjugates were purified by silica gel chromatography using 0-2% methanol in dichloromethane. ESI-MS for ADIBO-ATTO 647N: calculated $[M+H]^+$: 946.56; observed 946.29. ESI-MS for ADIBO-ATTO 655: calculated $[M+H]^+$: 827.34; observed 827.51.



DIBO-fluorescein diacetate

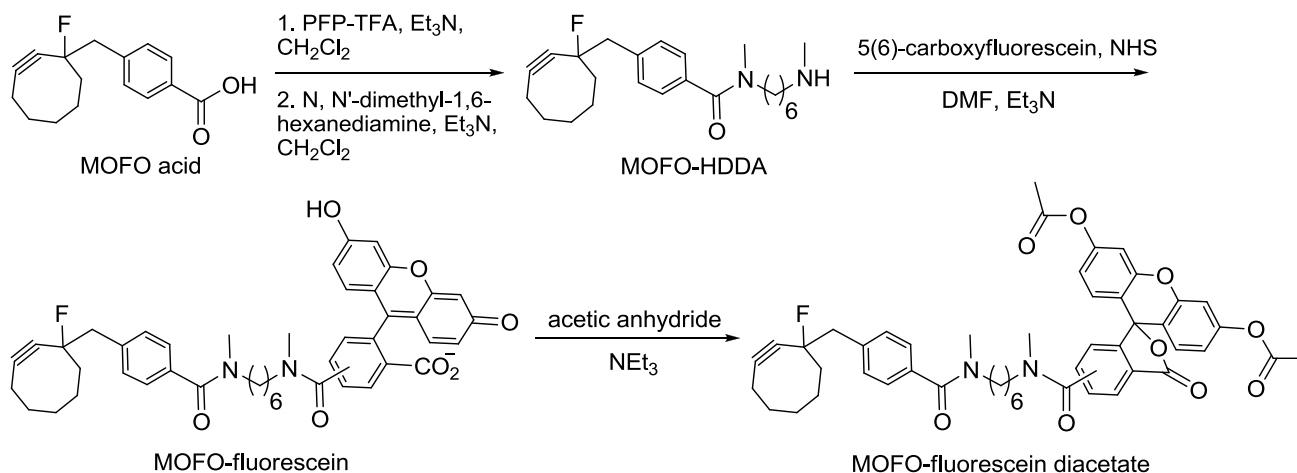
DIBO-fluorescein diacetate DIBO-fluorescein diacetate was synthesized in an analogous manner to ADIBO-fluorescein diacetate, from commercial DIBO-amine (Invitrogen) and fluorescein NHS ester (AnaSpec). The conjugate was purified by silica gel chromatography using 0-5% methanol in dichloromethane. ESI-MS for DIBO-fluorescein diacetate: calculated $[M+H]^+$: 763.22; observed 763.86.



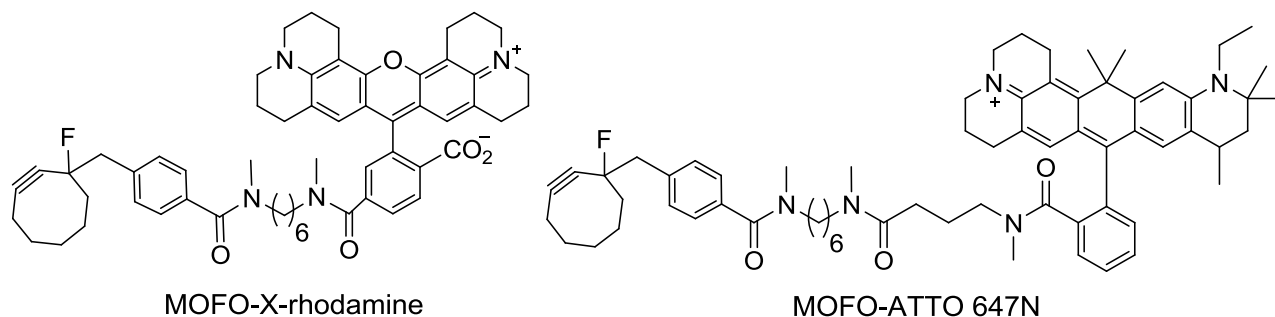
DIBO-Oregon Green 488 diacetate

DIBO-Oregon Green diacetate DIBO-Oregon Green 488 diacetate was a gift from Kyle Gee (Life Technologies).

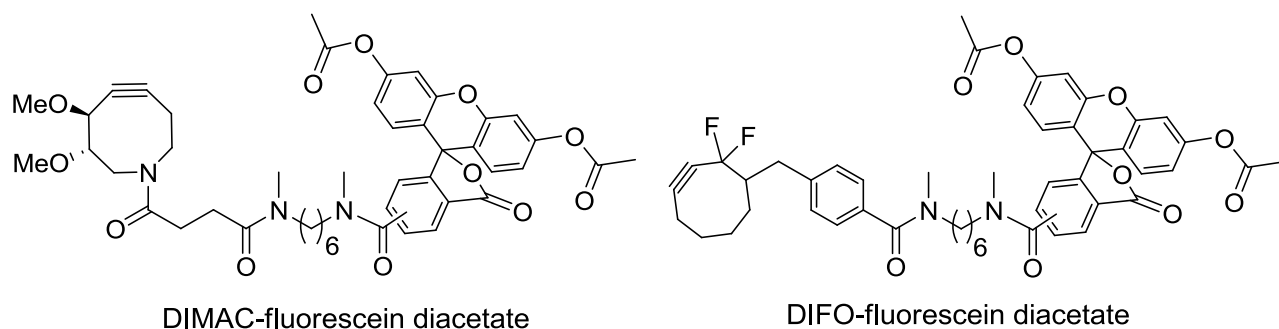
Synthesis of MOFO-, DIMAC-, and DIFO-fluorophore conjugates



MOFO-fluorescein diacetate To a solution of MOFO cyclooctyne acid² (5 mg, 19 μ mol) in 500 μ L anhydrous dichloromethane was added pentafluorophenyl trifluoroacetate (PFP-TFA, 9.8 μ L, 57 μ mol) and Et₃N (8 μ L, 57 μ mol). The reaction was allowed to proceed for 2 hr at room temperature. N, N'-dimethyl-1,6-hexanediamine (HDDA, 114 μ mol) was then added to the reaction mixture, which was allowed to stir for 5 hr at room temperature. Solvent was removed under reduced pressure. The reaction mixture was purified by silica gel chromatography (10-15% methanol in dichloromethane) to afford MOFO-N,N'-dimethyl-1,6-hexanediamine (MOFO-HDDA). MOFO-HDDA was dissolved in anhydrous DMF (300 μ L), and 5(6)-carboxyfluorescein, succinimidyl ester (9.8 mg, 20.9 μ mol) and Et₃N (8 μ L, 57 μ mol) were added to the mixture, which was allowed to stir for 10 hr at room temperature. Solvent was removed under reduced pressure. The residue was dissolved in a small amount of acetic anhydride (<200 μ L) and allowed to stir for 30 min at room temperature. After removal of acetic anhydride under reduced pressure, the reaction mixture was purified by silica gel chromatography (solvent gradient 0-5% methanol in dichloromethane) to afford MOFO-fluorescein diacetate (R_f = 0.4 in 10% methanol in dichloromethane). Estimated overall yield for four steps, 30-40%. ESI-MS for MOFO-fluorescein diacetate: calculated $[M+H]^+$: 829.34; observed 829.44.



MOFO-X-rhodamine, MOFO-ATTO 647N MOFO-HDDA was synthesized as described above, then conjugated to 5(6)-X-rhodamine NHS ester (Anaspec, 5(6)-ROX, SE) or ATTO 647N NHS ester (Sigma-Aldrich). Conjugates were purified by silica gel chromatography using 0-5% methanol in dichloromethane for MOFO-X-rhodamine and 0-2% methanol in dichloromethane for MOFO-ATTO 647N. ESI-MS for MOFO-X-rhodamine: calculated $[M+H]^+$: 903.49; observed 903.72. ESI-MS for MOFO-ATTO 647N: calculated $[M+H]^+$: 1014.66; observed 1014.42.



DIMAC-fluorescein diacetate, DIFO-fluorescein diacetate Fluorescein diacetate conjugates to DIMAC³ and DIFO⁴ were synthesized in a similar manner from their respective acids. Conjugates were purified by silica gel chromatography using 0-5% methanol in dichloromethane. ESI-MS for DIMAC-fluorescein diacetate: calculated $[M-H]^-$: 752.33; observed 752.40. ESI-MS for DIFO-fluorescein diacetate: calculated $[M+H]^+$: 847.33; observed 847.26.

Plasmids

For bacterial expression of LplA, we used His₆-LplA in pYFJ16.⁵ For mammalian expression of LplA, we used His₆-FLAG-LplA in pcDNA3.⁵ For mammalian expression of LAP fusion proteins, we used LAP-β-actin and LAP-MAP2 in Clontech vector,⁵ LAP-LDL receptor in pcDNA4, and LAP-neurexin-1β in pNICE. LAP-BFP expression constructs (LAP-BFP, LAP-BFP-NLS, LAP-BFP-CAAX, and LAP-BFP-NES) in pcDNA3 and LAP-mCherry in pcDNA3 were generated from corresponding pcDNA3-LAP-YFP plasmids⁵ by replacing YFP with BFP or mCherry, using the BamHI and EcoRI restriction sites. All LplA and LAP point mutants were prepared via QuikChange site-directed mutagenesis. Complete sequences of plasmids used in this study are available at <http://stellar.mit.edu/S/project/tinglabreagents/r02/materials.html> (Ting lab website).

Immunofluorescence staining of LplA (Figure S2B)

After live cell imaging, cells were fixed with 3.7% formaldehyde in Dulbecco's Phosphate Buffered Saline (DPBS) pH 7.4 for 10 min at room temperature followed by cold precipitation with methanol for 5 min at -20 °C, then blocked with 3% BSA in DPBS for 1 hr at room temperature. To visualize FLAG-tagged LplA, cells were incubated with 4 µg/mL mouse monoclonal anti-FLAG antibody (Sigma-Aldrich) in 1% BSA in DPBS for 1 hr at room temperature. Cells were further washed and incubated with 4 µg/mL goat anti-mouse IgG antibody conjugated to Alexa Fluor 568 (Life Technologies) in 1% BSA in DPBS for 1 hr at room temperature, then washed and imaged.

Kinetic analysis of azide 9 ligation (Figure S3C)

Reactions were set up as described in the main text. Aliquots were taken and quenched before product conversion exceeded 5%. To calculate initial rates, we determined the amount of product at each time point by generating a calibration curve using purified LAP and LAP-azide 9 mixed at different ratios. This curve correlated the measured ratio of integrated HPLC peak areas to the actual ratio, i.e. adjusted for any differences in extinction coefficient of LAP vs. LAP-azide 9. Initial rates (V_o) were determined at each azide 9 concentration, by plotting the amount of LAP-azide 9 product against time. The slope of the line gives V_o . V_o values were then plotted against azide 9 concentration in Figure S3C, and Origin 8.5.1 was used to fit the curve to the Michaelis-Menten equation $V_o = V_{max}[\text{azide 9}] / (K_m + [\text{azide 9}])$. From the V_{max} , k_{cat} was calculated using $V_{max} = k_{cat}[E]_{total}$. Measurements of V_o values at each azide 9 concentration were performed in triplicate.

Analysis of azide 7 and azide 9 ligation yields in cells (Figures 2C and S4A)

HEK cells were plated into wells of a 12-well culture plate (4 cm² per well) 18 hr prior to transfection and grown to 60% confluency. For azide 7 ligation, cells were transfected with 50 ng ^{WT}LplA and 1000 ng pcDNA3-LAP-YFP. For azide 9 ligation, cells were transfected with 500 ng ^{W37I}LplA and either 1000 ng pcDNA3-LAP-YFP or pcDNA3-LAP(K→A)-YFP using Lipofectamine 2000 (Life Technologies). The LplA:LAP plasmid ratios are identical to the conditions used for imaging in Figures 2B and S2B. 18 hr after transfection, cells were incubated in growth media (MEM supplemented with 10% FBS) containing 200 µM azide 7 or azide 9 for 30 min or 1 hr at 37 °C. Excess azide probe was washed out over 1 hr. Cells were then harvested and

lysed in 500 μ L hypotonic lysis buffer (1 mM HEPES pH 7.5, 5 mM $MgCl_2$, 1 mM PMSF (Thermal Scientific, phenylmethanesulfonyl fluoride), 1 mM protease inhibitor cocktail (Sigma-Aldrich)), frozen at -20 $^{\circ}C$, thawed at room temperature, then mixed by vortexing for 2 min. This freeze-thaw-vortex cycle was repeated three times. Cells were then centrifuged at 13,000 rpm for 2 min, and the supernatant was analyzed on a 12% polyacrylamide native gel without SDS (5 μ L lysate per lane) at constant 200 V. Prior to Coomassie staining, in-gel fluorescence of YFP was visualized on a FUJIFILM FLA-9000 instrument using LD473 laser and Long Pass Blue (LPB) filter. A repeat of the experiment in Figure 2C gave ligation yields of 67% for WT LplA (50 ng plasmid) + azide 7, and 89% for W371 LplA (500 ng plasmid) + azide 9 (data not shown).

Analysis of two-step ligation yield after strain-promoted cycloaddition in cells (Figure S4B)

HEK cells plated into wells of a 12-well culture plate (4 cm^2 per well) were transfected with 500 ng pcDNA3- W371 LplA and 1000 ng pcDNA3-LAP-mCherry using Lipofectamine 2000 (Life Technologies). Azide 9 labeling and washout were performed in the same manner as in Figure S4A. After excess azide 9 washout, cells were incubated in MEM containing 10 μ M DIBO-biotin (Life Technologies) for 10 min at 37 $^{\circ}C$. Thereafter, cells were further washed for 2.5 hr to remove excess DIBO-biotin. Cells were then harvested and lysed in the same manner as in Figure S4A. The cell lysate was incubated with 5 μ M of streptavidin for 1 hr at 4 $^{\circ}C$, then analyzed on a 12% SDS-polyacrylamide gel at constant 200 V, under conditions known to preserve biotin-streptavidin binding as well as streptavidin's subunit association.⁶ Prior to Coomassie staining, in-gel fluorescence of mCherry was visualized on FUJIFILM FLA-9000 instrument using SHG532 laser and Long Pass Green (LPG) filter.

Cell fixation after live cell DIMAC-fluorescein and DIFO-fluorescein labeling (Figure S5A)

After live cell imaging, cells were fixed with 3.7% formaldehyde in DPBS pH 7.4 for 10 min at room temperature followed by cold precipitation with methanol for 5 min at -20 $^{\circ}C$. Cells were then washed with DPBS several times over 10 min, before imaging.

Cell surface and intracellular labeling with commercial DIBO conjugates (Figure S6)

DIBO-Alexa Fluor 647 cell surface labeling (Figure S6A)

HEK cells plated on glass coverslips in wells of a 48-well cell culture plate (0.95 cm² per well) were transfected with 100 ng pcDNA4-LAP-LDL receptor or 400 ng pNICE-LAP-neurexin-1 β using Lipofectamine 2000. At 18 hr after transfection, cells were washed three times with MEM. Enzymatic ligation of azide 9 on the cell surface was performed in MEM with 5 μ M ^{W371}Lp1A, 500 μ M azide 9, 2 mM ATP and 2 mM magnesium acetate for 20 min at room temperature (to minimize internalization of cell-surface proteins). After washing three times with MEM, cells were incubated with 10 μ M DIBO-Alexa Fluor 647 in MEM for 10 min at room temperature. Cells were then washed three times with MEM and imaged live.

DIBO-biotin cell surface and intracellular labeling (Figure S6A, S6B)

DIBO-biotin cell surface labeling was performed in the same manner as DIBO-Alexa Fluor 647 cell surface labeling, described above. After DIBO-biotin incubation, cells were washed three times with DPBS and fixed with 3.7% formaldehyde in DPBS pH 7.4 for 10 min at room temperature, followed by cold precipitation with methanol for 5 min at -20 °C. Fixed cells were then blocked with 1% casein in DPBS for 1 hr at room temperature. To visualize specific labeling, cells were stained with streptavidin conjugated to Alexa Fluor 568 or Alexa Fluor 647 in 0.5% casein in DPBS for 5 min at room temperature, followed by washing three times with DPBS and imaging.

For DIBO-biotin intracellular labeling, HEK cells plated on glass coverslips in wells of a 48-well cell culture plate (0.95 cm² per well) were transfected with 400 ng pcDNA3-LAP-BFP-NLS and 200 ng pcDNA3-^{W371}Lp1A. Azide 9 labeling/washout and DIBO-biotin labeling/washout were performed in the same manner as in Figure S4B. After DIBO-biotin washout, cells were fixed and stained with streptavidin-Alexa Fluor 568, as described above.

Quantitative analysis of fluorophore-cyclooctyne labeling specificity (Figures 3B and 5B)

Cells with signal at least 3-fold greater than autofluorescence from untransfected cells in the cyclooctyne channel were selected by hand for analysis. For each of these cells, one region in the cytosol (representing background) and one region in the nucleus (representing specific signal) were manually circled. The background-corrected mean fluorescence intensity was determined for both regions using SlideBook. Excel was used to plot the nuclear versus cytosolic fluorescence intensity for each cell. Since ATTO 647N labeling signal was low, we selected for analysis cells with signal at least 2-fold greater than autofluorescence from untransfected cells in the ATTO 647N channel.

Quantitative analysis of MOFO-fluorescein labeling of LAP-BFP using four LplA mutant/azide substrate pairs (Figure S2A)

Cells with fluorescein signal at least 2-fold greater than autofluorescence from untransfected cells, and BFP signal at least 5-fold greater than autofluorescence were selected by hand for analysis. For each of these cells, the entire area of the cell representing signal was circled. SlideBook was used to calculate the mean intensities in both channels. The background-corrected mean fluorescein intensity was plotted against the background-corrected mean BFP intensity using Excel.

Quantitative analysis of LplA mutant expression levels in cells (Figure S2C)

Cells with Alexa Fluor 568 signal at least 1.5-fold greater than background (area without any cell) were selected by hand for analysis. For each of these cells, the entire area of the cell representing signal was circled. SlideBook was used to calculate the mean intensities in the channel. The background-corrected mean Alexa Fluor 568 intensity was plotted using Excel.

Other protocols

LplA and mutants were expressed and purified as previously described.⁵ The 13-amino acid LAP peptide ($\text{H}_2\text{N-GFEIDK}\underline{\text{V}}\text{WYDLDA-CO}_2\text{H}$)⁷ was synthesized by the Tufts University Peptide Synthesis Core Facility and purified to >96% homogeneity.

Reference List

1. Kuzmin,A.; Poloukhine,A.; Wolfert,M.A.; Popik,V.V. *Bioconjugate Chemistry* **21**, 2076-2085 (2010).
2. Agard,N.J.; Baskin,J.M.; Prescher,J.A.; Lo,A.; Bertozzi,C.R. *Acs Chemical Biology* **1**, 644-648 (2006).
3. Sletten, E.M.; Bertozzi,C.R. *Org. Lett.* **10**, 3097-3099 (2008).
4. Codelli,J.A.; Baskin,J.M.; Agard,N.J.; Bertozzi,C.R. *Journal of the American Chemical Society* **130**, 11486-11493 (2008).

5. Uttamapinant, C.; White, K.A.; Baruah, H.; Thompson, S.; Fernandez-Suarez, M.; Puthenveetil, S.; Ting, A.Y. *Proceedings of the National Academy of Sciences of the United States of America* **107**, 10914-10919 (2010).
6. Howarth, M.; Chinnapen, D.J.; Gerrow, K.; Dorrestein, P.C.; Grandy, M.R.; Kelleher, N.L.; El-Husseini, A.; Ting, A.Y. *Nature Methods* **5**, 397-399 (2008).
7. Puthenveetil, S.; Liu, D.S.; White, K.A.; Thompson, S.; Ting, A.Y. *Journal of the American Chemical Society* **131**, 16430-16438 (2009).
8. Los, G.V.; Encell, L.P.; McDougall, M.G.; Hartzell, D.D.; Karassina, N.; Zimprich, C.; Wood, M.G.; Learish, R.; Ohana, R.F.; Urh, M.; Simpson, D.; Mendez, J.; Zimmerman, K.; Otto, P.; Vidugiris, G.; Zhu, J.; Darzins, A.; Klaubert, D.H.; Bulleit, R.F.; Wood, K.V. *Acs Chemical Biology* **3**, 373-382 (2008).